Pseudoscalar Meson Electroproduction Above the Resonance Region

Bogdan B. Niczyporuk

Jefferson Lab, Newport News, VA 23606, USA

presented
at
CLAS with 6 GeV Beams Workshop, January 12-13, 1999

Abstract

One principal motivation for studying exclusive reactions is that they provide a new class of observables, called off-diagonal parton distributions, for the internal structure of the nucleon. The study of exclusive reactions provides a probe of nucleon structure complementary to purely inclusive studies. The simplest, and possibly the most promising, type of experiment is exclusive electroproduction of pseudoscalar mesons at small t, and at large Q^2 and W. We show that using the CLAS spectrometer at JLAB and with beam energies between 4 and 6 GeV, we can obtain good quality electroproduction data that will improve our understanding of nucleon structure.

1. Physics Motivations

The structure of the nucleon revealed in hard processes is described by parton distributions. Traditionally, the internal structure of the nucleon has been studied (CERN, SLAC, DESY) through inclusive scattering of high energy leptons in the deep inelastic scattering (DIS) limit, i.e. at large Q^2, ν, and fixed Bjorken $x = Q^2/2m_p\nu$, where Q^2 and ν are the mass squared and energy of the virtual photon. For example, unpolarized DIS provided the first evidence that quarks carry only about 45% of the nucleon momentum via measurements of the structure function $F_1(x, Q^2)$, or the corresponding parton densities $q(x, Q^2)$. Recent measurements have focused on the leading-twist structure function $g_1(x, Q^2)$, which is roughly proportional to the inclusive spin asymmetry on a longitudinally polarized target. Polarized DIS measurements of $g_1(x, Q^2)$, or the relevant helicity densities $\Delta q(x, Q^2)$, have revealed that only about 30% of the nucleon's spin is carried by the quark's intrinsic spin [1].

Processes where at least one hadron is detected in the final state offer several distinct advantages over inclusive processes alone [2], and references therein. Particularly interesting is the chirally odd structure function $h_1(x, Q^2)$, or the appropriate transversity densities $\delta q(x, Q^2)$ [3, 4]. Together with $F_1(x, Q^2)$ and $g_1(x, Q^2)$, $h_1(x, Q^2)$ is necessary for a complete description of the quark structure of the nucleon in high-energy processes. The structure function $h_1(x, Q^2)$ has never been measured. Chirally odd quark distributions are difficult to measure because they are suppressed in totally inclusive deep inelastic scattering. However, the asymmetry for semi-inclusive leptoproduction of pions off transversely polarized target contains a contribution from $h_1(x, Q^2)$ that is enhanced at low x. Another motivation for the measurement of $h_1(x, Q^2)$ is a sensitivity to the role of relativistic effects in the nucleon state, and a possible sensitivity [2] to gluon contributions to the spin of the proton.

Exclusive electroproduction of mesons from nucleons has become a field of growing interest [5, 6, 7] since a full factorization theorem has been proved [8, 9, 10]. It has been shown that exclusive meson production at large Q^2 and small t factorizes into a hard scattering coefficient, a quark-antiquark distribution amplitude of the meson, and an off-diagonal quark (or gluon) distribution that describes the "soft" physics in the nucleon. The proof of factorization applies when the virtual photon is longitudinally polarized. It has been also shown [8] that transverse polarization of the photon implies a power suppression in Q relative to the case of longitudinal polarization. The theorem applies to the production of mesons at all x. Therefore, off-diagonal (also called off-forward [9] or non-forward [10]) parton distributions allow the description of certain exclusive reactions in the framework of QCD.

For longitudinally polarized vector mesons, the relevant parton densities are the unpolarized ones, $q(x, Q^2)$. For transversely polarized vector mesons, the parton densities are the quark transversity densities, $\delta q(x, Q^2)$. The original hope [8] that $h_1(x, Q^2)$ may be measured via production of transverse vector mesons has, unfortunately, not come true because in hard scattering processes such a transition is forbidden [11, 12]. For the pseudoscalar mesons, the relevant parton densities are the

quark helicity densities, $\Delta q(x, Q^2)$, which are not suppressed at large x. Hence, the polarized parton densities can be probed in unpolarized collisions.

It is clear that the study of exclusive and semi-inclusive reactions provides a probe of nucleon structure complementary to purely inclusive studies. In particular, we should study exclusive reactions at low t, and at high Q^2 and W, in the region of validity of QCD factorization theorems, and also in the transition region where standard partonic model may no longer be valid. One can then probe in a novel way the soft part of a proton, and elucidate the transition between soft and hard scattering processes.

A measurement of the differential cross section $\sigma(t, W, Q^2)$ for the reactions $e^- + p \rightarrow e^- + \pi^+(K^+) + n(\Lambda^o)$ at beam energies 4.0, 4.5, 5.0, 5.5 and 6.0 GeV was proposed and discussed [13]. Data will be collected simultaneously for π^+, π^o and K^+ exclusive electroproduction using the CLAS detector at JLAB in the following kinematical region: $Q^2 > 1\ GeV^2$ and $W > 2\ GeV$. In the following sections existing data, cross section, detailed simulation, reconstruction and analysis of charged pions electroproduction will be discussed.

2. Cross Section

The procedure of extracting a virtual photon cross section $\sigma_{\gamma_v p}$ from the observed electroproduction cross section is based on the one-photon approximation. In this procedure electrons are regarded as providing a beam of virtual photons (flux Γ) of known polarization ϵ, mass squared Q^2, and energy ν. Electroproduction reactions can be described in terms of form factors that are generalizations of the form factors observed in elastic electron-proton scattering, or in terms of cross sections that are extensions of the photoproduction cross sections. The most general form of the differential cross section σ for the reactions

$$e^- + p \rightarrow e^- + \pi^+(K^+) + n(\Lambda^o) \tag{1}$$

can be written in terms of four structure functions (unpolarized data) [14]:

$$\sigma_{\gamma_v p}(W^2, Q^2, t, \phi) \quad = \quad \sigma_T + \epsilon\sigma_L + \epsilon\sigma_{TT}cos2\phi + \sqrt{\epsilon(\epsilon+1)/2} \cdot \sigma_{LT}cos\phi \tag{2}$$

where σ_T, σ_L, σ_{TT}, and σ_{LT} are functions of the variables: Q^2, $W^2 = 2m_p\nu - Q^2 + m_p^2$, and $t \equiv (p_{\gamma_v} - p_{\pi,K})^2 - t_{min}$ (or θ^*, the angle between the virtual photon and the meson in the hadronic center of mass W). The dependence on the azimuthal angle ϕ (angle of the meson relative to the electron scattering plane: $\phi \equiv \phi^*$) is shown explicitly in eq. (2). The parameter ϵ is the polarization of the virtual photon $\epsilon = [4E_{beam}(E_{beam}-\nu)-Q^2]/[4E_{beam}(E_{beam}-\nu)+2\nu^2+Q^2]$. The term σ_T represents the cross section for transverse photons, σ_L represents the cross section for longitudinal photons, σ_{TT} is the interference between the transverse amplitudes, and σ_{LT} is the interference between transverse and longitudinal amplitudes. The terms σ_{TT} and σ_{LT} approach zero as $t \rightarrow 0$, and the terms σ_L and σ_{LT} vanish as $Q^2 \rightarrow 0$. In eq. (2),

the structure functions σ_T and σ_{TT} can be further decomposed into two parts: $\sigma_\perp$ corresponds to incident photons polarized perpendicular to the hadronic plane, and $\sigma_\parallel$ corresponds to photons polarized parallel to the hadronic plane: $\sigma_T = (\sigma_\parallel + \sigma_\perp)/2$, $\sigma_{TT} = (\sigma_\parallel - \sigma_\perp)/2$ and $\sigma_{LT} = 2Re(A_L A_\parallel^*)$.

Transversely polarized target. In eq. (2) we took explicitly into account the helicities of the virtual photon and ignored the helicities of ingoing and outgoing nucleon [14]. By taking into account the nucleon spin, $\sigma_\parallel = |A_\parallel^N|^2 + |A_\parallel^F|^2$, $\sigma_\perp = |A_\perp^N|^2 + |A_\perp^F|^2$, $\sigma_L = |A_L^N|^2 + |A_L^F|^2$, and $\sigma_{LT} = 2Re(A_L^N A_\parallel^{N*} + A_L^F A_\parallel^{F*})$, where N and F refer to nucleon flip and non-flip amplitudes, respectively. In the t channel, the contributions to $A_\perp^{N,F}$ come only from natural parity exchange, and contributions to $A_\parallel^{N,F}$ and $A_L^{N,F}$ come only from unnatural parity exchange. Using a transversely polarized target one obtains six more structure functions which are the imaginary parts of products of non-flip and flip amplitudes $Im(A_i^N A_j^{F*})$.

Determination of the pion form factor from electroproduction data requires the extraction of that part of the cross section which contains the spin-flip amplitudes, i.e. $|A_\parallel^F|^2$ and $|A_L^F|^2$.

The "inverse" reaction to $\gamma p \to \pi^+ n$ is the $\pi^+ n \to \rho^o p$. Good quality data [15] exist only for the reaction $\pi^- p \to \rho^o n$ at 17.2 GeV. The measured differential cross section, for the above reaction, as a function of $\sqrt{t}$ shows a behavior one would expect for one-pion exchange mechanism (spin flip amplitude) which vanishes at $t = 0$. The most interesting observation for the $\pi^- p \to \rho^o n$ reaction is the presence of strong polarization effects [16], i.e. a large left-right polarized target asymmetry (presence of non-flip amplitudes) in the low t region. A sizable asymmetry was also observed [17] in π^+ photoproduction from a polarized target at 5 and 16 GeV. A typical value of the asymmetry is about -0.5 in both experiments. This is very surprising since, according to general belief, this region should be dominated by one-pion exchange and should, therefore, show little or no polarization effects.

3. Simulation

We have used the SDA Package [18] to simulate the $ep \to e\pi^+(K^+)n(\Lambda^o)$ reactions and to reconstruct the events accepted in the CLAS detector. In order to estimate rates we have used the following form for the differential cross sections [20]:

$$\frac{d^2\sigma}{dQ^2 dW} = \frac{\alpha W \sqrt{(W^2 + Q^2 - m_p^2)^2 + 4m_p^2 Q^2}}{\pi(1-\epsilon)(s - m_p^2)^2 Q^2} \cdot \frac{d\sigma_{\gamma v p}(W, Q^2, \theta^*, \phi^*)}{d\Omega_{\pi,K}} \tag{3}$$

where the first term is a flux Γ of virtual photons, the second term, $\sigma_{\gamma v p}$, represents the four structure functions as shown by eq. (2), and s is the center-of-mass energy squared $s = m_p^2 + 2m_p E_{beam}$.

In our simulation we have used the measured cross section $\sigma_{\gamma v p}$ at $Q^2 < 1$ GeV^2 [21] and extrapolated to higher Q^2 values with a simple pole form: $\sim (1 + Q^2/0.462)^{-2}$.

A sample of 1.6 million events was generated in the Q^2 range from 1.2 to 3.2 GeV^2 and in W range from 2.05 to 2.15 GeV for 5 beam energies: 4.0, 4.5, 5.0, 5.5 and 6.0 GeV. Realistic trajectories of charged particles traversing the CLAS magnetic field were simulated, including multiple scattering and the drift cell spatial resolution of 250μm. For the purpose of the present study, both the scattered electron and the meson had to be detectable in the trigger scintillation counters and in all layers of the drift chambers in a given sector. Additionally, we required that the outgoing electron is within the acceptance of the Čerenkov and Shower Counters. These requirements (acceptance) provide optimal trajectory reconstruction for both charged particles, and also a good missing mass resolution.

Hereafter, we refer to the number of the generated events weighted by the cross section (see eq.(3)) at a given luminosity as the number of produced events, N_{prod}. A fraction of the N_{prod} events that would have been accepted by the geometry of the CLAS detector is not observed because of reconstruction inefficiencies and various other losses like: decaying pions (kaons), secondary interactions, radiative corrections, missing mass cut, etc. These losses depend on the event kinematics and can be corrected for on an event-by-event bases [19]. In the present study, to account for these losses, we have introduced a constant global weight factor $w_g = N_{acc}/N_{obs} = 1.4$.

During the reconstruction process we assumed that opposite sectors of the CLAS detector are not perfectly aligned, but are rotated relative to each other randomly by an angle of 1 mrad. We also have assumed that each nominal beam energy is randomly off by 0.1%. The W, Q^2, and t regions were chosen to obtain sufficient acceptance for at least 4 of the beam energies.

Rates. In Table 1, using eq. (3), we show the expected rates of produced N_{prod} and fully reconstructed N_{obs} events with a run of 100 hours/E_{beam} of the CLAS detector at a luminosity $L = 10^{34}cm^{-2}s^{-1}$ for $\Delta W = 2.05 - 2.15$ GeV and $\Delta\Omega_\pi = 2\pi \int sin\theta_\pi^* d\theta_\pi^* = 0.377sr$ ($\theta_\pi^* < 20^o$). The analysis of the CLAS data taken at a beam energy of 4 GeV shows that the rates for semi-inclusive electroproduction of charged pions are approximately larger by a factor of 15.

4. Particle Identification

To identify scattered electrons we first determine the clusters in the Shower Counter. Negative tracks (potential electrons) which match these clusters are selected. These tracks are then checked to determine whether the deposited energy in the cluster agrees with the track momentum. For our kinematical conditions, outgoing mesons have momenta ranging from 2.0 to 3.5 GeV, therefore the Time-of-Flight technique is not adequate. Hence, the outgoing mesons are identified using a missing mass technique. Our preliminary analysis of 4 GeV CLAS data indicate that the background under the missing mass peak of the neutron is only about a few percent.

5. Analysis of Reconstructed Events

From the reconstructed (observed) events N_{obs}, we extract the Q^2 and t (or θ^*) dependence of the structure functions: σ_T, σ_L, σ_{TT} and σ_{LT} in a model independent

way. The procedure consists of fitting the form of the differential cross section in eq. (3) to the measured cross sections in a given kinematical bin $\Delta Q^2 \Delta W \Delta t$. The structure functions $\sigma_T + \epsilon \sigma_L$, σ_{TT} and σ_{LT} can be isolated experimentally using the ϕ dependence of the cross section at a given beam energy. A separation of σ_T and σ_L requires data measured at different beam energies.

The measured cross section $(\partial \sigma_{\gamma v p}/\partial \vec{k})_m$ has been obtained from $N_{obs} \pm \sqrt{N_{obs}}$ in each bin $\Delta \vec{k} = \Delta Q^2 \Delta W \Delta \theta^* \Delta \phi^*$ in the following way:

$$\left(\frac{\partial \sigma_{\gamma v p}}{\partial \vec{k}} \right)_m = \frac{N_{obs}(\Delta \vec{k}) \cdot w_g(E_b)_m}{A(\Delta \vec{k}, E_b) \cdot L_m(E_b) \cdot F_m(\Delta W, \Delta Q^2, E_b) \cdot \Delta \vec{k}_m} \tag{4}$$

The average acceptance $A_m(\Delta \vec{k}, E_b)$ in each bin $\Delta \vec{k}$ and at each beam energy has been determined by generating at random 400 events/bin. These events were transformed into the lab system with a random rotation of the electron scattering plane around the beam direction, and were checked to determine if the outgoing electron and meson both lie within the geometry of the CLAS detector [19]. In Table 2, as an example, we show the acceptance as a function of the c.m. angles $(\theta_\pi^*, \phi_\pi^*)$ for $\Delta W = (2.05 - 2.15) \ GeV$, $\Delta Q^2 = (2.0 - 2.2) \ GeV^2$ and $E_{beam} = 4.5 \ GeV$. The measured flux $F_m(\Delta W, \Delta Q^2, E_b)$, in eq. (4), was obtained by averaging over all events observed in a bin $\Delta W \Delta Q^2$ and for given beam energy. In Fig. 1 we show, as an example, the derived differential cross sections as a function of ϕ^* and E_{beam} for one bin k of size $\Delta W \Delta Q^2 \Delta t$.

To extract the four structure functions from the measured cross sections in a bin k, as shown in Fig. 1, we used the following functional form in the χ^2 minimization procedure:

$$f(\phi^*)_k = \sum_i \left(P_1 + P_2 \cdot \epsilon_i + P_3 \cdot \epsilon_i \cdot cos2\phi^* + P_4 \cdot \sqrt{\epsilon_i(\epsilon_i + 1)/2} \cdot cos\phi^* \right) \tag{5}$$

where the index i runs over the different beam energies.

The four parameters (P_1, P_2, P_3, and P_4) are determined from the fit. The virtual photon polarization ϵ_i was evaluated at the center of the ΔW and ΔQ^2 bins. Data with $A(\Delta \vec{k}, E_b) < 2\%$ were excluded from the fit, see Table 1. The Q^2 dependence of the four structure functions and their statistical errors, derived from the fits, are summarized in Fig. 2 for pions only (see full circles with error bars). The dashed or solid curves in Fig. 2 represent the input to the Monte Carlo simulation. The full squares and the stars in Fig. 2 represent the currently available data [22]. The fitting procedure also includes the expected systematic errors in determining the luminosity $L_m(E_b)$ of $\leq 1\%$ and a global correction $w_g(E_b)_m$ of $\leq 2\%$; i.e., uncorrelated systematic errors at each beam energy setting. In addition to the above, we introduced a correlated systematic error (common to all beam energies) of about 3%. The succesfull σ_L and σ_T separation was possible, in the above kinematical regions, once sufficient data were collected for at least 4 of the 5 beam energies.

6. Summary

A challenging problem in particle physics is to understand the transition from the "current" quarks and gluons appearing in the QCD Lagrangian to the degrees of freedom of low-energy QCD. One could take the approach that anything that can be calculated by pQCD can be called a hard process. All the rest would be soft. Soft interactions are usually understood as the interactions of hadrons at a relatively small scale (low Q^2 in ep interactions or low p_T in hadron-hadron interactions). The problem, however, is that what we calculate and what we measure are not the same. Soft interactions are not easily disentangled from hard ones [23].

That said, let us summarize here what we can measure in a model independent way.

Stage 0. Analyze the existing data taken at a beam energy of 4 GeV. Extract the Q^2 and t dependences of the structure functions: $\sigma_T + \epsilon\sigma_L$, σ_{TT}, and σ_{LT}.

Stage 1. Take new data at beam energies: 4.5, 5.0, 5.5 and 6.0 GeV, and now disentangle the σ_L and σ_T cross sections.

Stage 2. Measure, for the first time, asymmetries for exclusive and semi-inclusive electroproduction on transversely polarized target. Technically, it is a challenging task to operate CLAS with the strong transverse magnetic field of a polarized target.

Conclusion

We have shown that using the CLAS spectrometer at JLAB and with beam energies between 4 and 6 GeV, we can obtain good quality electroproduction data that will improve our understanding of the nucleon structure as well as the hadronic properties of the photon. We emphasize the importance of studying both the Q^2 and t dependencies of the various structure functions for π^+, π^o and K^+ exclusive electroproduction. In order to access higher W and Q^2 at higher beam energies, we need to design a new large acceptance detector in the forward direction.

Acknowledgments

References

[1] S. D. Bass, TUM/T39-99-03, hep-ph/9902280.

[2] J.M. Niczyporuk and E.E.W. Bruins, Phys. Rev. D **58**, 91501 (1998).
J.M. Niczyporuk, S. B. thesis, Massachusetts Institute of Technology, 1977 (available at http://www-hermes.desy.de/~dilys/pub/97-LIB/nicz.97.018.ps.gz).

[3] R.L. Jaffe and X. Ji, Phys. Rev. Lett. **71**, 2547 (1993).

[4] Xiangdong Ji, Phys. Rev. D **49**, 114 (1994).

[5] M. Vanderhaeghen, M. Guidal, and J.M. Laget, Phys. Rev. C **57**, 1454 (1998).

[6] L. Mankiewicz, G.Piller and A. Radyushkin, TUM/T39-98-33, hep-ph/9812467.

[7] S.J. Brodsky, M. Diehl, P. Hoyer and S. Peigne, SLAC-PUB-8015, hep-ph/98122277.

[8] J.C. Collins, L. Frankfurt and M. Strikman, Phys. Rev. D **56**, 2982 (1997).

[9] X. Ji, Phys. Rev. Lett. **78**, 610 (1997); Phys. Rev. D **55**,7114 (1997).

[10] A.V. Radyushkin, Phys. Rev. D **56**, 5524 (1997).

[11] P. Hoodbhoy and X. Ji, Phys. Rev. D **58**, 054006 (1998).

[12] M. Diehl, T. Gousset and B. Pire, Phys. Rev. D **59**, 034023 (1998).

[13] B.B. Niczyporuk, "Workshop on CEBAF at Higher Energies", CEBAF, Newport News, April 14-16, 1994. (see also Abstract submitted to Baryons'95, Santa Fe, 3-7 October 1995).

[14] A. Bartl and W. Majerotto, Nucl. Phys. B **62**, 267 (1973).

[15] G. Grayer, B. Hyams *et al.*, Nucl. Phys. B **75**, 189 (1974).

[16] H. Becker, G. Blanar *et al.*, Nucl. Phys. B **151**, 46 (1979).

[17] C.C. Morehouse, M. Borghini *et al.*, Phys. Rev. Lett. **25**, 835 (1970).

[18] B.B. Niczyporuk, "Standard Data Analysis (SDA) Package" (unpublished), CEBAF-PR-91-004 (1991).

[19] B.B. Niczyporuk, CEBAF-PR-89-040 (1989).

[20] R.G. Roberts, "The Structure of the Proton", Cambridge University Press, 1990.

[21] C.N. Brown, C.R. Canizares *et al.*, Phys. Rev. D **8**, 92 (1973).

[22] C.J. Bebek, C.N Brown *et al.*, Phys. Rev. D **17**, 1693 (1978).
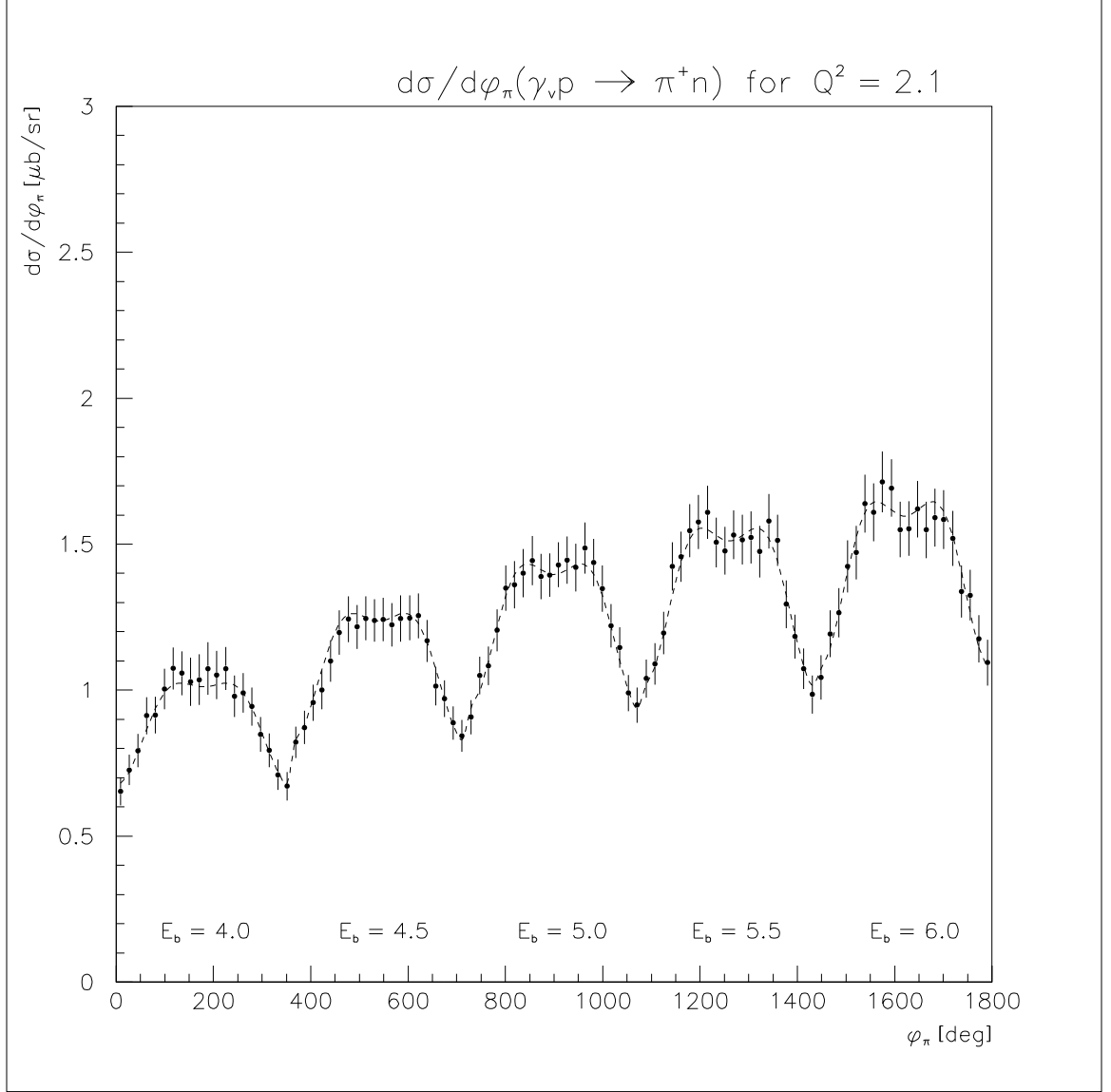
[23] A. Levy, DESY-95-204, hep-ex/9511006.

Figure 1: An example of the derived differential cross section as a function of ϕ^* and E_{beam} for $Q^2 = 2.1 \ GeV^2$.

$$d\sigma/dQ^2(\gamma_v p \rightarrow \pi^+ n)$$

$<W> = 2.1$ GeV and $\Theta^*_\pi < 20°$
($\Delta W = 0.1$ and $\Delta Q^2 = 0.2$)

$E_{beam} = 4.0, 4.5, 5.0, 5.5$ and 6.0 GeV
(100hr/E_{beam} at $L=10^{34}$ s^{-1}cm^{-2})

● This Proposal
Curves $\propto (1 + Q^2/0.462)^{-2}$
P.R. D8 1973, p.92

Bebek et al., P.R. D17 (1978)1693
$(W,Q^2)= (2.15,1.2), (2.65,2.0), (2.65,3.3)$
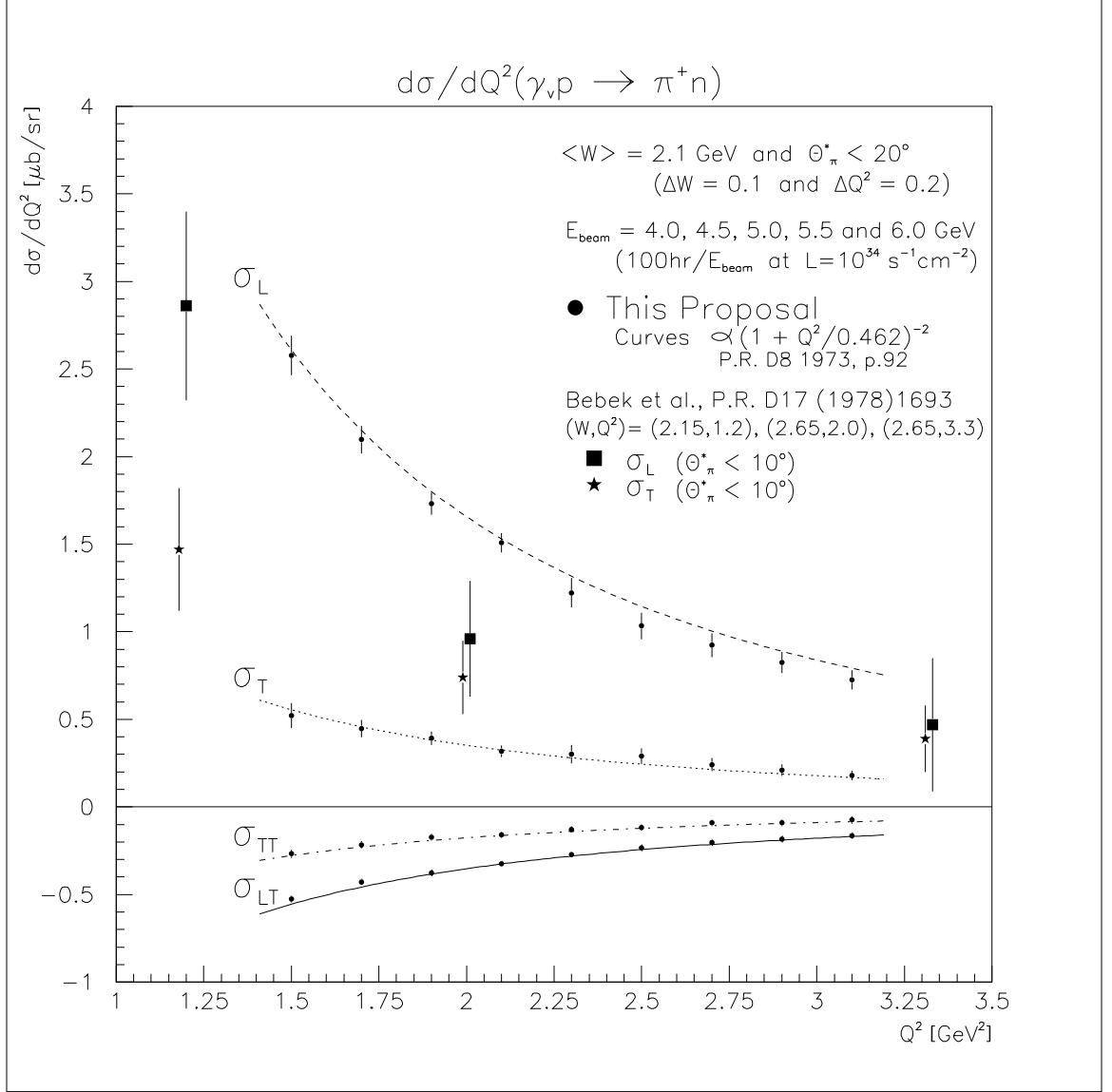■ σ_L ($\Theta^*_\pi < 10°$)
★ σ_T ($\Theta^*_\pi < 10°$)

Figure 2: The Q^2 dependence of the four structure functions and their statistical errors, derived from fits, for pions. Existing data [22]: σ_L ($\square$) and σ_T ($\star$)

10

Table 1: Expected rates of produced (N_{prod}/100hr) and reconstructed (N_{obs}/100hr) π^+ mesons using the CLAS detector at a luminosity of $10^{34}cm^{-2}s^{-1}$ for $\Delta W = (2.05 - 2.15)$ GeV and $\Delta\Omega_\pi = 0.377sr$ ($\theta_\pi^* < 20^o$).

ΔQ^2	$E_b = 4.0$ N_{prod} N_{obs}	$E_b = 4.5$ N_{prod} N_{obs}	$E_b = 5.0$ N_{prod} N_{obs}	$E_b = 5.5$ N_{prod} N_{obs}	$E_b = 6.0$ N_{prod} N_{obs}
1.4 - 1.6	36349 13226	43455 13547	49217 11511	53913 6677	
1.6 - 1.8	23494 8946	28537 10395	32698 10073	36107 8091	38980 5059
1.8 - 2.0	15564 5968	19372 7566	22451 7755	25049 7283	27130 5957
2.0 - 2.2	10527 3918	13480 5440	15805 5999	17756 5975	19441 5343
2.2 - 2.4	7262 2552	9545 3987	11399 4533	12926 4692	14175 4511
2.4 - 2.6		6881 2855	8325 3494	9571 3738	10511 3678
2.6 - 2.8		5011 2017	6196 2645	7182 2942	8012 3016
2.8 - 3.0		3682 1419	4670 1994	5472 2311	6144 2457
3.0 - 3.2		2734 974	3541 1487	4219 1792	4779 1960

Table 2: An example of the acceptance as a function of the c.m. angles $(\theta_\pi^*, \phi_\pi^*)$ for $\Delta W = (2.05 - 2.15)\ GeV$, $\Delta Q^2 = (2.0 - 2.2)\ GeV^2$ and $E_{beam} = 4.5\ GeV$.

$\Delta\phi_\pi^*\ [^o]$	$\Delta\theta_\pi^*\ [^o]$ 0 - 5	$\Delta\theta_\pi^*\ [^o]$ 5 - 10	$\Delta\theta_\pi^*\ [^o]$ 10 - 15	$\Delta\theta_\pi^*\ [^o]$ 15 - 20
0 - 18	0.72	0.70	0.67	0.68
18 - 36	0.67	0.69	0.64	0.63
36 - 54	0.68	0.66	0.57	0.51
54 - 72	0.64	0.54	0.53	0.48
72 - 90	0.64	0.59	0.48	0.45
90 - 108	0.64	0.55	0.45	0.39
108 - 126	0.68	0.52	0.43	0.39
125 - 144	0.70	0.58	0.46	0.41
144 - 162	0.64	0.60	0.52	0.44
162 - 180	0.63	0.66	0.60	0.42
180 - 198	0.67	0.61	0.57	0.41
198 - 216	0.66	0.60	0.56	0.41
216 - 234	0.64	0.55	0.44	0.34
234 - 252	0.64	0.55	0.49	0.36
252 - 270	0.63	0.52	0.50	0.45
270 - 288	0.67	0.59	0.52	0.43
288 - 306	0.67	0.61	0.54	0.46
306 - 324	0.69	0.63	0.53	0.56
324 - 342	0.73	0.69	0.66	0.59
342 - 360	0.68	0.71	0.66	0.70